JJEE
Volume 2, Number 2, 2016
Pages 94-106
Jordan Journal of Electrical Engineering
ISSN (Print): 2409-9600, ISSN (Online): 2409-9619

Spanner-Shaped Ultra-Wideband Monopole Antenna with Bluetooth and GSM Coverage

Shaimaa' Naser[a], Nihad Dib[b]

Department of Electrical Engineering, Jordan University of Science and Technology, Irbid, Jordan
[a]e-mail: naser.shaimaa@yahoo.com
[b]e-mail: nihad@just.edu.jo

Received: January 20, 2016 *Accepted: March 9, 2016*

Abstract— In this paper, the design and analysis of a compact size microstrip ultra-wideband (UWB) antenna is considered. The antenna is mounted on a 38 mm× 25 mm cheap FR4 substrate of dielectric constant ε_r= 4.4 and thickness of 1.6 mm. The original shape of the patch is circular; and a hexagonal notch is removed (making it a spanner-shaped antenna) to achieve ultra-wideband characteristics. To cover the Bluetooth and the GSM 1800 bands, a meandered strip is integrated with the spanner-shaped antenna. Also, the antenna has super-wideband characteristics with an upper frequency edge of 50 GHz. To reject the interference from WiMAX (3.5 GHz) and WLAN (5.5 GHz), two slots are etched from the radiating patch. The antenna has a stable Omni-directional radiation pattern and a peak gain that increases in the UWB range from 2 dBi to 10 dBi, while it is almost 0.7 dBi at the GSM 1800 center frequency and 1.65 dBi at the Bluetooth center frequency. Measurements show a good agreement with the simulated results which are obtained using HFSS simulator.

Keywords— Multi-band antennas, Printed antennas, Super-wideband antenna, Ultra-wideband (UWB) antennas.

I. INTRODUCTION

In 2002, the FCC has adopted the band 3.1-10.6 GHz and a power spectral density of -41.3 dBm/MHz for the use of unlicensed ultra-wideband (UWB) communication [1] which was the largest spectrum allocation for unlicensed communications ever granted. Since then, many studies have been performed on the design of UWB antennas. There are many types of UWB antennas in the literature, but, recently, most researchers have been focusing on the design of printed monopole antennas broad bandwidth, low cost, and low profile.

Modern wireless devices are designed to support different applications which operate at different frequency bands. Due to the space limitation, it is difficult to place an antenna for each application. Hence, using an antenna that operates at different frequency bands has a great advantage of reducing the overall size of devices. A coplanar waveguide fed antenna for quad-band applications was presented in [2]. The quad-band operation was achieved through imposing various current paths in a modified T-shaped radiating element. The antenna covered GSM 900, DCS 1800, IEEE802.11.a, IEEE802.11.b and HiperLAN-2 bands. In [3], a dual band planar monopole antenna for WLAN applications was proposed. The antenna has the shape of the letter omega, and uses the self-similarity property to exhibit dual band characteristics. In [4], a microstrip-fed printed dual band antenna for Bluetooth and ultra-wide band applications with WLAN (5.15–5.825 GHZ) band-notch characteristics was proposed. The desired dual band characteristic was obtained by using a spanner-shaped monopole with rectangular strip patch, whereas the band-notch characteristic was created by a mushroom-like structure. A coupled-line-fed planar ultra-wideband (UWB) antenna was proposed in [5]. It has band-notched characteristics at 3.5 GHz and 5.5 GHz using bent resonators as well as two integrated monopoles designed for covering GSM 900 MHz and Bluetooth 2.4 GHz.

Corresponding author's e-mail: naser.shaimaa@yahoo.com

Currently, the trend is to have super-wideband antennas to serve the long and short range future communications that require very large bandwidth including the UWB range. In [6], a clover structured monopole antenna for super-wideband applications was proposed. The antenna has a wide impedance bandwidth from 1.9 GHz to frequency over 30 GHz. In [7], a planar microstrip-fed super-wideband monopole antenna was proposed. By embedding a semi-elliptically fractal-complementary slot into the asymmetrical ground plane, a 10-dB bandwidth from 1.44-18.8 GHz was achieved. In [8], an octagonal fractal microstrip patch antenna was proposed to operate from 10 GHz to 50 GHz frequency range.

In this paper, a super-wideband spanner-shaped antenna is proposed. Besides, a super-wideband antenna covers the Bluetooth and GSM 1800 bands. Simulations are performed using HFSS simulator [9] to reach the proposed design. The rest of the paper is organized as follows: section II describes the structure of the proposed antenna and final optimized parameter; section III presents different frequency domain and time domain parameters of the proposed UWB antenna; and section IV considers a parametric study of different parameters that affect the performance of the antenna. Finally, section V concludes and summarizes the paper.

II. ANTENNA DESIGN

The structure of the proposed spanner-shaped antenna along with the optimized parameters is illustrated in Fig. 1. It is placed on top of an FR4 substrate of $\varepsilon_r = 4.4$ and compact dimensions of 25 mm× 38 mm× 1.6 mm. A partial ground plane is used to have the UWB characteristics, whereas the corners of the ground plane are chamfered to improve the impedance bandwidth. The antenna is fed through a 50Ω microstrip line of dimensions 3 mm×12 mm. The distance between the feeding point and the ground plane ($L_{feeding} - L_{gnd}$) influences the return loss of the antenna. So, a value of 0.2 mm is chosen to have a good return loss in the whole band. UWB coverage is obtained through the spanner-shaped patch which evolves from a circular monopole of radius of 11.5 mm, while the GSM 1800 (1.82-1.865 GHz) and the Bluetooth (2.38-2.49 GHz) coverages are obtained through the meandered strip. Switching between Bluetooth and GSM 1800 bands is obtained by controlling the length of the meandered strip using a switch having dimensions of 1 mm× 1 mm. Usually, a PIN diode is used as a switch for high switching purposes. The initial length of the meandered strip was evaluated to be $\lambda/4$ at the desired center frequency (1.842 GHz for the GSM 1800 band and 2.442 GHz for the Bluetooth), which was computed to be 40.7 mm for the GSM 1800 and 30.7 mm for Bluetooth. Then, several simulations were performed to optimize the lengths which were somewhat different from the calculated values due to the parasitic effects of the corners of the meandered strip. When the switch is in the ON state (short circuit), the total length of the meandered strip is 55 mm and covers the GSM 1800 band. However, when the switch is in the OFF state (open circuit), the length of the meandered strip is 27.5 mm and covers the Bluetooth band. A U-shaped slot and a straight slot are inserted in the patch to reject the interference from WiMAX (3.3-3.8 GHz) and WLAN (5-5.9 GHz), respectively. The initial lengths of these slots were set to be λ/2 at the center frequency of the intended band (26 mm for the WiMAX and 16.6 mm for the WLAN). Then, the total lengths and widths were varied to get the optimized values [10].

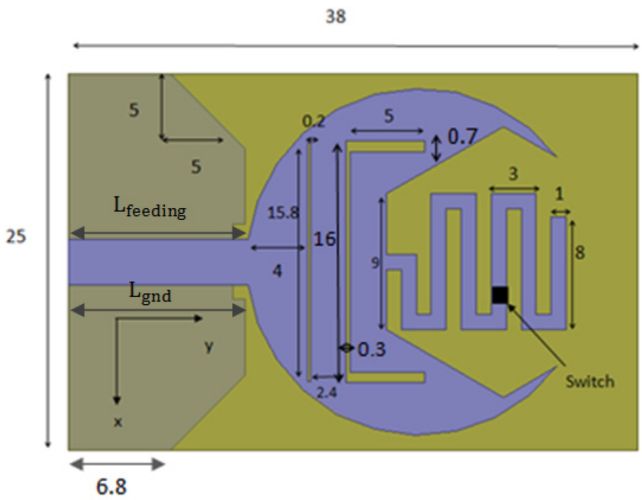

Fig. 1. The structure of the proposed spanner-shaped antenna. All dimensions are in millimeters

III. Antenna Parameters

The optimized antenna dimensions were used to build a prototype of the proposed antenna. Fig. 2 illustrates the fabricated prototypes of the antenna for both switch states. The simulated and measured voltage standing wave ratio (VSWR), which is a measure of the impedance matching of the proposed antenna for both switch states, is illustrated in Fig. 3. Measurements were performed in the laboratory environment using Agilent vector network analyzer (VNA). It can be seen that measurements agree with simulation except in the band 11-13 GHz, which could be due to connectors. When the switch is OFF, the antenna covers the Bluetooth range and the UWB range with a VSWR value less than 2. On the other hand, when the switch is in the ON state, the antenna covers the GSM 1800 range and the UWB range. Additionally, the antenna has notch characteristics around 3.5 and 5.5 GHz with a small shift caused by the variation of the dielectric constant at high frequencies [11]. Fig. 4 shows the simulated reflection coefficient (in dB) in an extended frequency range (0-50 GHz). It can be noticed that the antenna has a better return loss (which is the difference in dB between the incident power and the reflected power) than 10 dB up to 50 GHz except in the narrowbands 18-19.5 GHz and 37-39 GHz. Thus, the antenna has a super-wideband characteristic which makes it a good candidate for applications that need very large bandwidths in the future.

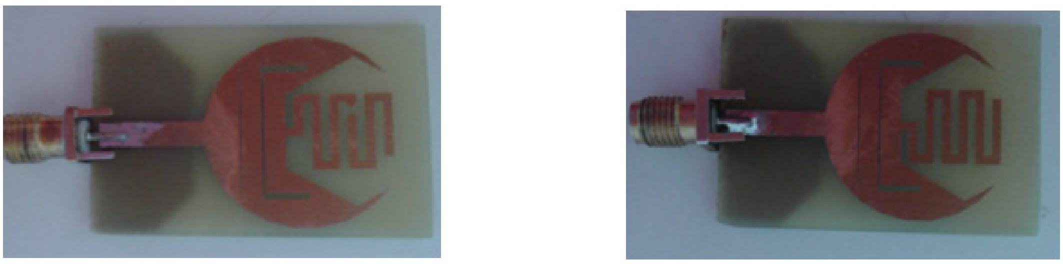

(a) (b)

Fig. 2. The prototypes of the spanner-shaped antenna when the switch in: a) OFF state, b) ON state

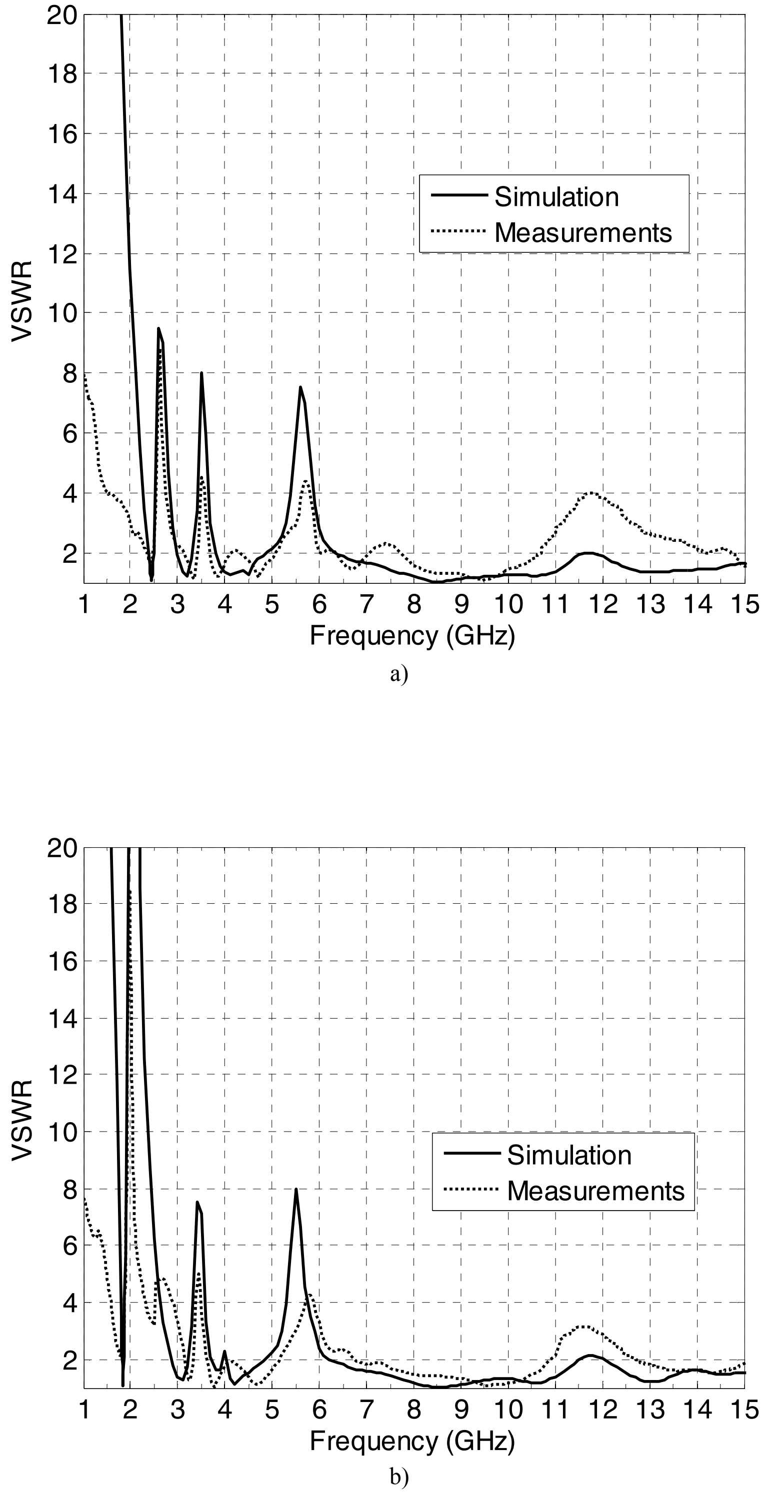

Fig. 3. The simulated and measured VSWR when the switch is a) OFF, b) ON

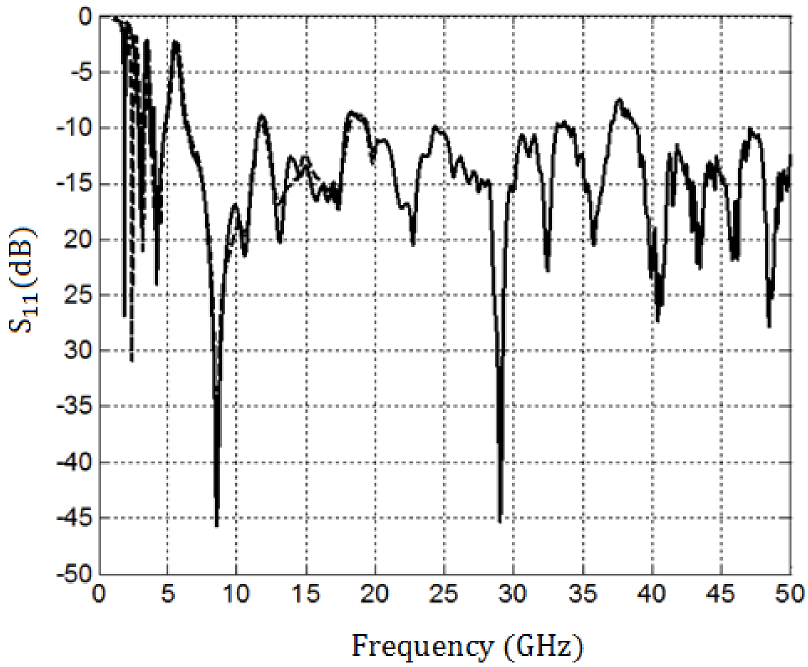

Fig. 4. The simulated S_{11} (in dB) up to 50 GHz: solid line: switch is ON; dashed line: switch is OFF

The simulated co-polarization and cross-polarization radiation patterns in the E-plane (*yz*-plane) and the *H*-plane (*xz*-plane) of the proposed antenna at different frequencies are illustrated in Figs. 5 and 6, respectively. In Fig. 5, the *E*-plane has almost the shape of number 8 at all frequencies with a small cross-polarization component, but as the frequency increases the pattern becomes distorted due to the increased effect of the higher order modes. Also, it is clear that the back radiation in terms of the co-polarization and cross-polarization is high due to the effect of using partial ground plane. In Fig. 6, the antenna is almost Omni-directional in the *H*-plane at low frequencies with cross-polarization component lower than the co-polarization one, but as the frequency increases, the pattern becomes distorted and the cross-polarization component increases for the same reasons mentioned before.

To further study the antenna behavior, the current distribution at 1.842, 2.442, 3.5, 5.5 GHz is shown in Fig. 7. Fig. 7a indicates that when the switch is OFF, the current is highly distributed at the feeding line and the meandered strip portion that is responsible for the Bluetooth coverage. In Fig. 7b, when the switch is ON, the current is also mainly distributed at the feeding line and along the whole length of the meandered strip. To study the effect of the notches, Fig. 7 shows the current distribution at 3.5 GHz and 5.5 GHz. Based on figs. 7c and 7d, one can notice that the two notches have filter characteristics at the desired bands since the current is mainly concentrated at them. Finally, the current distribution at 9 GHz, which lies within the UWB range, is shown in Fig. 8. It is clear that the current is highly distributed at the spanner-shaped patch edges and the feeding line.

Another frequency domain parameter is the realized peak gain which is illustrated in Fig. 9 for both states. It can be seen that the antenna (in both states) has a maximum gain of 10 dBi and a gain of 1 dBi and 2 dBi at 1.842 GHz and 2.442 GHz, respectively, while it drops to -6 dBi and -3 dBi at 3.5 GHz and 5.5 GHz, respectively.

Finally, the group delay is considered to study the dispersion of the antenna. Fig. 10 illustrates the measured and simulated group delay using S_{11} for both switch states. The group delay for both states is almost fixed in the whole band, which indicates a very small dispersion caused by the antenna.

IV. PARAMETRIC STUDY

In this section, a study of different parameters that affect the antenna performance will be presented. The parameters considered in this section are: the side length of the hexagon, the chamfered edges dimensions of the ground plane, and the length of the meandered strip for both states of the switch. In this section, the effect of the notches is not considered, so all the parametric studies are performed without the notches.

Fig. 11 illustrates the effect of changing the side length of the hexagon. It is clear that the side length has a large effect on the return loss of the antenna. A value of 9 mm was chosen to have the low frequency edge at 3.1 GHz and good return loss through the band. Next, the effect of varying the dimensions of the chamfered edges is considered. Fig. 12 shows that chamfering the edges improves the return loss. Suitable dimensions were chosen to be 5 mm×5 mm.

The effect of the meandered strip length when the switch is in the ON state is illustrated in Fig. 13a. As the length of the meandered strip increases, the center frequency decreases. A length of 55 mm was chosen to have the resonance at 1.842 GHz (center frequency of GSM 1800). Moreover, Fig. 13b shows the effect of varying the length of the meandered strip that is responsible for the Bluetooth coverage when the switch is OFF. A value of 27.5 mm was chosen to have the resonance at 2.442 GHz (the center frequency of Bluetooth).

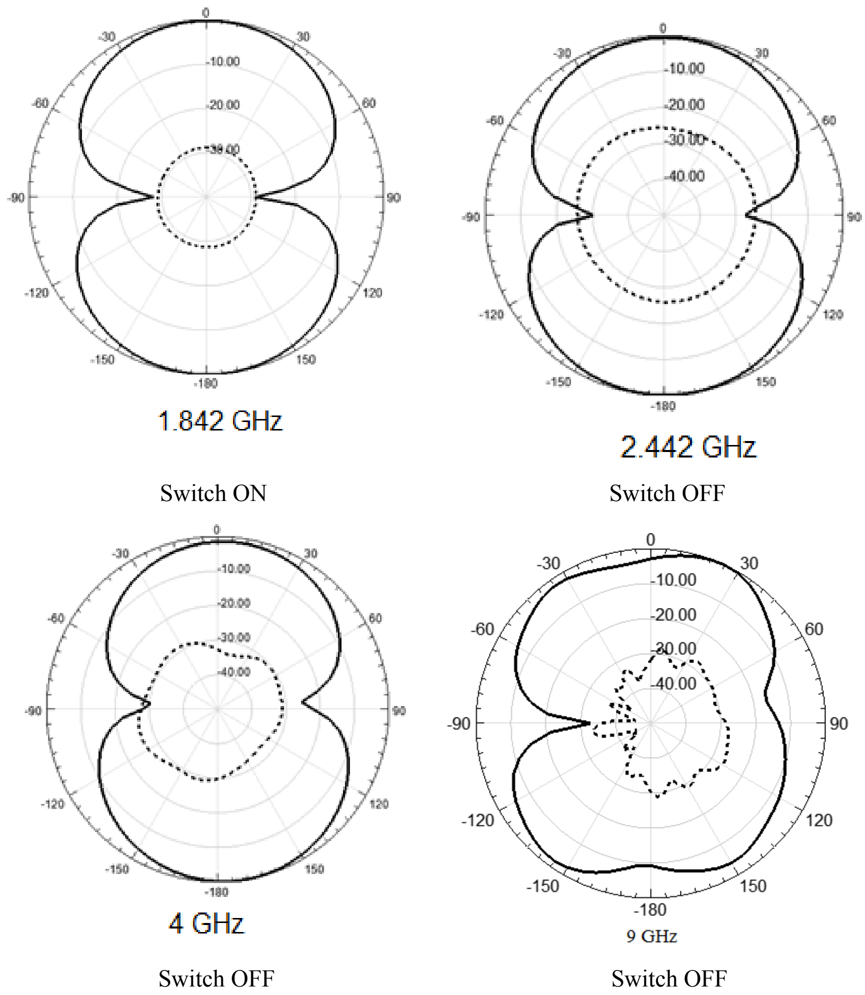

Fig. 5. The simulated co-polarization (solid line) and cross-polarization (dashed line) *E*-plane patterns of the proposed spanner-shaped antenna

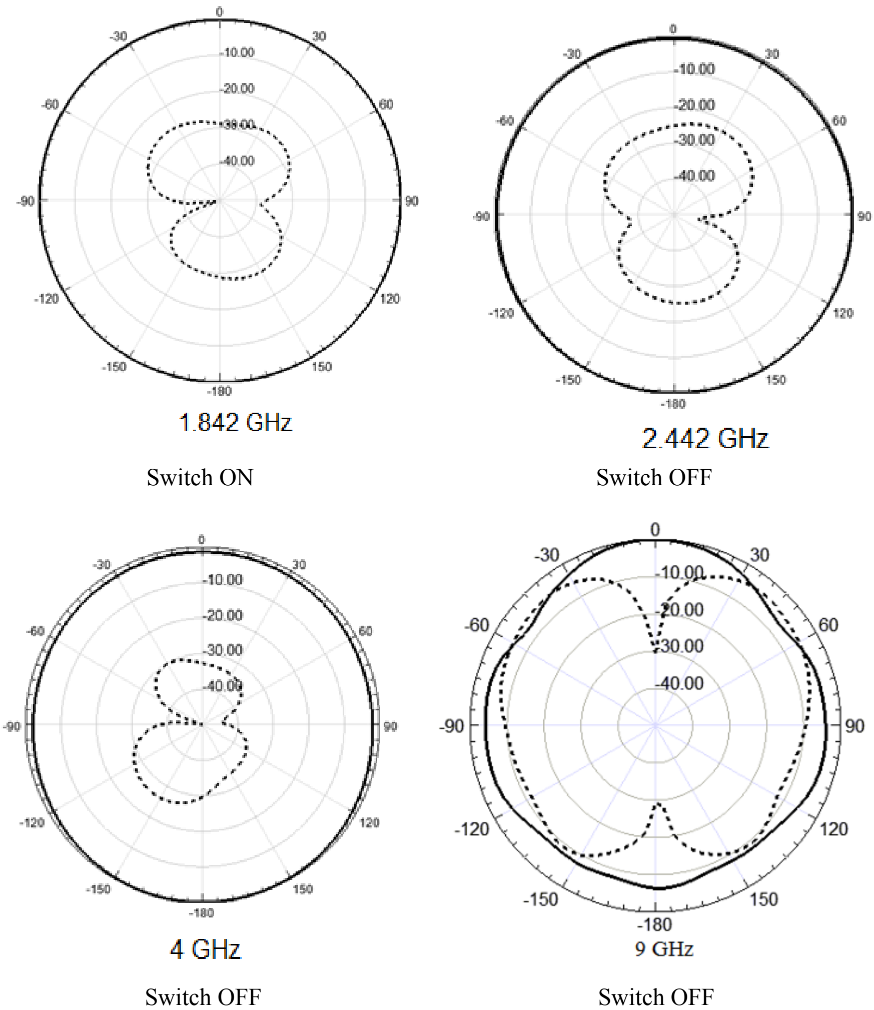

Fig. 6. The simulated co-polarization (solid line) and cross-polarization (dashed line) H-plane patterns of the proposed spanner-shaped antenna

Table 1 lists a comparison between the proposed antenna and other ones that have recently appeared in the literature. It can be seen that the proposed design has a comparable size to others, with larger peak gain. Moreover, the low and high frequency edges compete with the ones cited in the table with maximum frequency edge of 50 GHz.

TABLE 1
COMPARISON BETWEEN THE PROPOSED AND PREVIOUS DESIGNS

Reference Number	Dimensions	Peak Gain (dBi)	Low Frequency Edge (GHz)	High Frequency Edge (GHz)
[8]	60 mm× 60 mm	9	10	50
[12]	40 mm×40 mm	2.9	2.9	11
[13]	30 mm×30 mm	4	3.2	12
[14]	42 mm× 40 mm	4.4	2.44	11.9
[15]	25 mm×20 mm	3	2.63	13.02
[16]	41 mm× 34 mm	4.85	3.26	19.1
[17]	63.25 mm×51 mm	-	3.1	15
[18]	30 mm×40 mm	-	2.2	12
[19]	30 mm×35.5 mm	-	2.9	>10
[20]	31 mm×45 mm	7	2.18	44.5
Spanner-shaped antenna	38 mm×25 mm	10	2.9	50

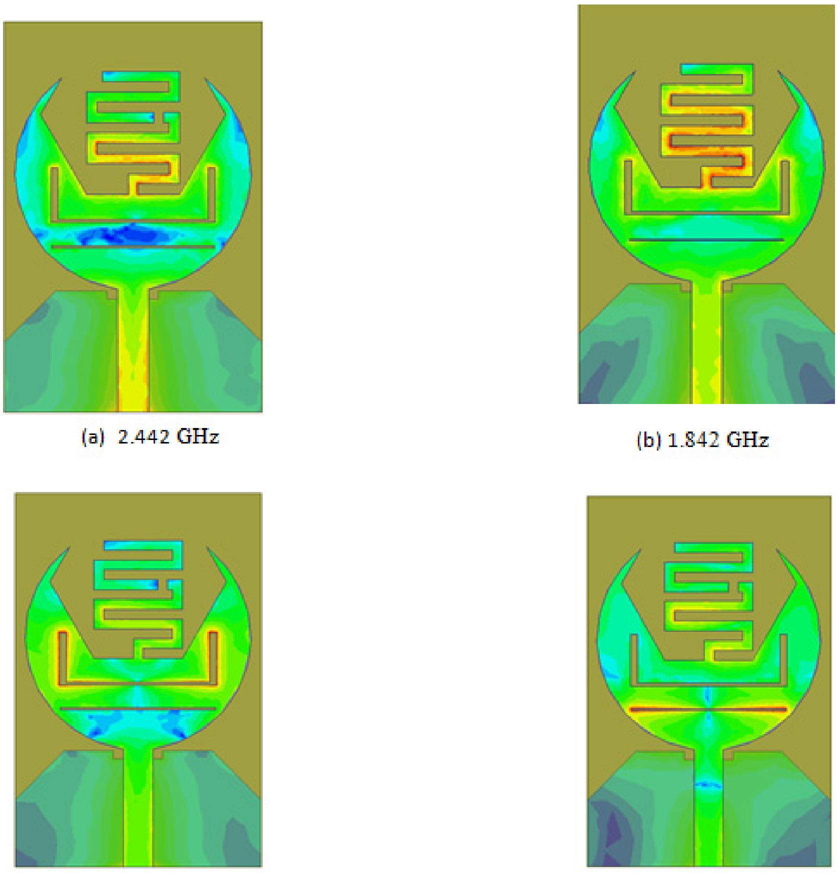

(a) 2.442 GHz

(b) 1.842 GHz

(c) 3.5 GHz

(d) 5.5 GHz

Fig. 7. The current distribution at 1.842, 2.442, 3.5 and 5.5 GHz

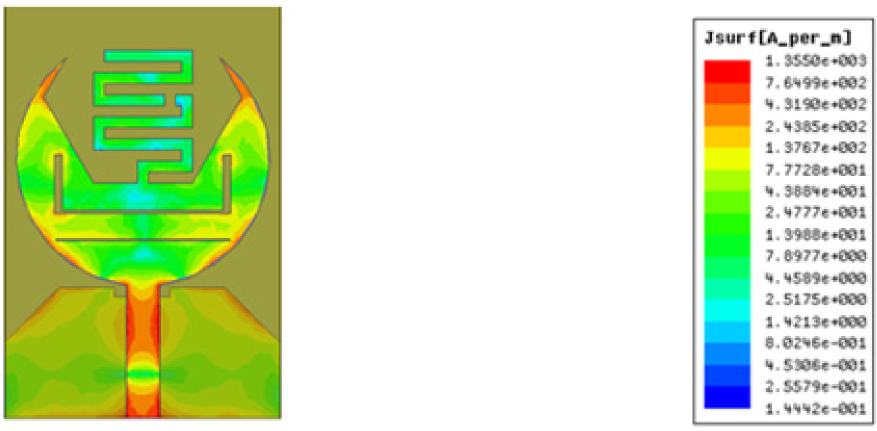

Fig. 8. The current distribution at 9 GHz

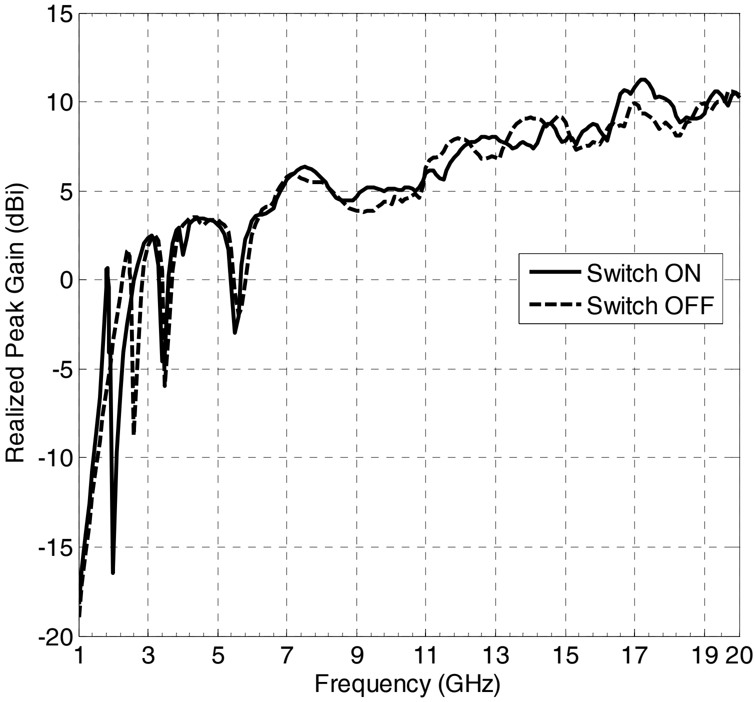

Fig. 9. The simulated realized peak gain of the proposed spanner-shaped antenna for both switch states

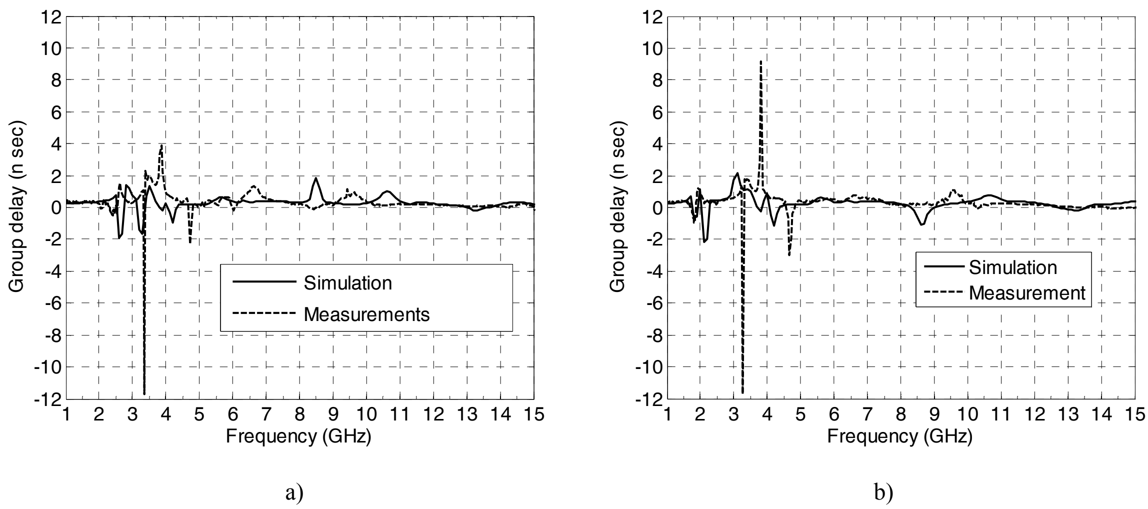

Fig. 10. The simulated and measured group delay for the a) OFF state, b) ON state

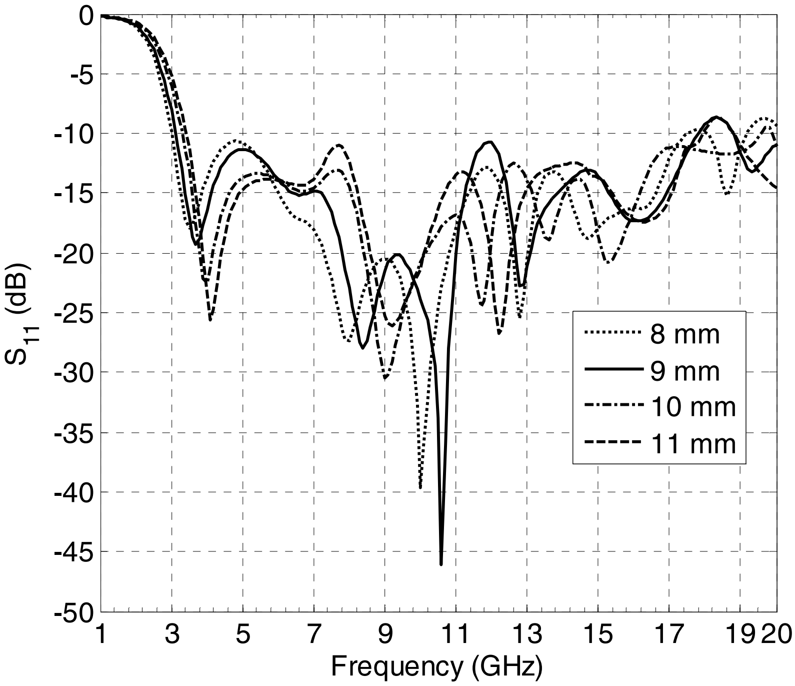

Fig. 11. The effect of varying the side length of the hexagon

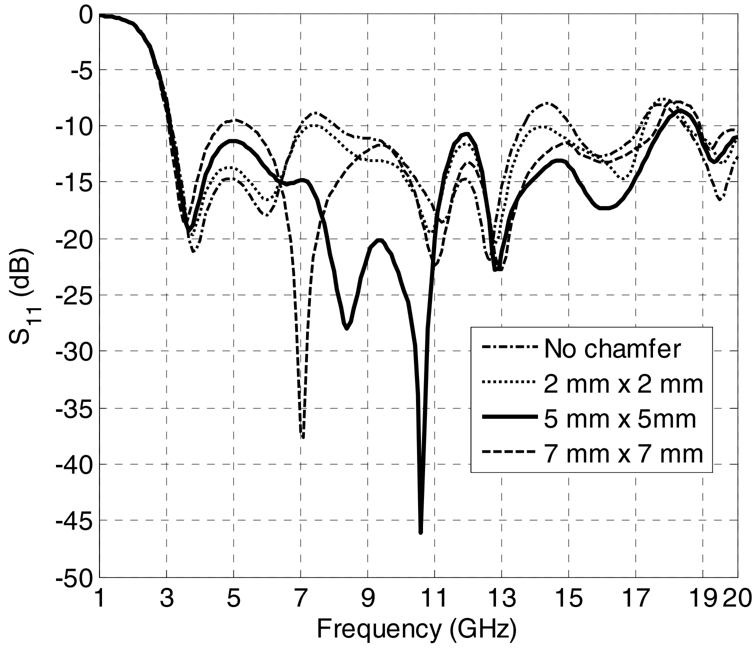

Fig. 12. The effect of varying the dimensions of the chamfered edges of the ground plane

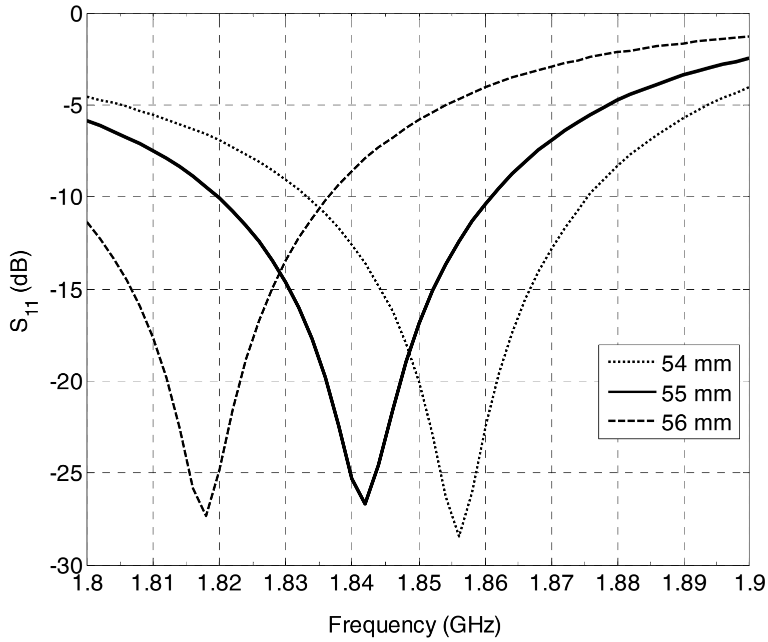

a)

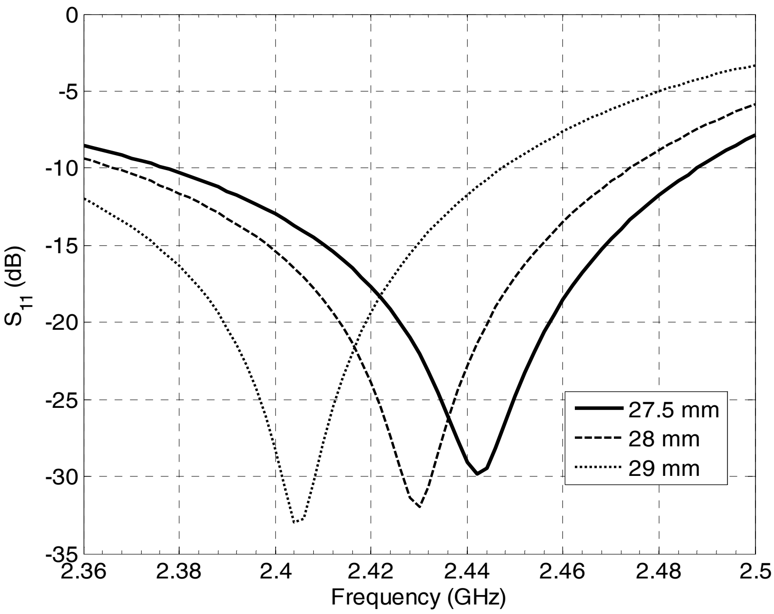

b)

Fig. 13. The effect of varying the length of the meandered strip when the switch is: a) ON, b) OFF

V. CONCLUSION

In this paper, a compact printed UWB spanner-shaped monopole antenna with two additional bands and two band-notched frequencies was designed and analyzed. Simulations showed that the antenna works well in the UWB range with better than 10 dB return loss. Moreover, the antenna has super-wideband characteristics with an upper frequency edge of 50 GHz. Additionally, the antenna works at another two bands: Bluetooth and GSM 1800. To reject the interference from WiMAX (3.5 GHz) and WLAN (5.5 GHz), two slots in the radiating patch were used. Experimental results were very close to the simulation ones. Frequency domain and time domain characteristics were investigated. The antenna exhibits a stable Omni-directional radiation pattern with high peak gain except at the notched frequencies. Also, the group delay of the antenna, which was almost constant, indicated that the distortion caused by the antenna is very small except at the notched frequencies. As a future work, combining two proposed UWB antennas to form two ports UWB MIMO antenna to improve the reliability of the signal and capacity will be investigated.

REFERENCES

[1] Federal Communications Commission, *First Report and Order, Revision of Part 15 of Commission's Rule Regarding UWB Transmission System FCC 02-48*, Washington, USA, 2002.

[2] R. Sujith, V. Deepu, S. Mridula, B. Paul, D. Laila and P. Mohanan, "Compact CPW-fed uniplanar antenna for multiband wireless applications," *International Journal of Electronics and Communications*, vol. 65, pp. 553-559, 2011.

[3] K. Sayidmarie and T. Nagem, "Compact dual-band dual-omega printed monopole antenna for WLAN applications," *Proceeding of Jordan International Electrical and Electronic Engineering Conference*, pp. 1-6, 2013.

[4] T. Mandal and S. Das, "Design of a microstrip fed printed monopole antenna for bluetooth and UWB applications with WLAN notch band characteristics," *International Journal of RF and Microwave Computer-Aided Engineering*, vol. 25, no. 1, pp. 66-74, 2015.

[5] A. Khalilzadeh, A. Tan and K. Rambabu, "Design of an integrated UWB antenna with dual band notch characteristics," *International Journal of Electronics and Communications,* vol. 67, no.5, pp. 433-437, 2013.

[6] S. Palaniswamy, M. Kanagasabai, S. Kumar, M. Alsat, S. Velan and J. Pakkathillam, "Super wideband printed monopole antenna for ultra wideband applications," *International Journal of Microwave and Wireless Technologies*, available on CJO2015, doi:10.1017/S1759078715000951.

[7] K. R. Chen, C. Sim and J. Row, "A compact monopole antenna for super wideband applications," *IEEE Antennas and Wireless Propagations Letters*, vol. 10, pp. 488-491, 2011.

[8] A. Azari, "A new super wideband fractal microstrip antenna," *IEEE Transactions on Antennas and Propagation*, vol. 59, no. 5, pp. 1724-1727, 2011.

[9] *ANSYS-High Frequency Structure Simulator (HFSS)*, Ansys Inc., 2011.

[10] J. Zang and X.Wang, "A compact c-shaped printed uwb antenna with band-notched characteristic," *Progress in Electromagnetics Research Letters*, vol. 43, pp. 15-23, 2013.

[11] S. Mumby and J. Yuan, "Dielectric properties of FR-4 laminates as a function of thickness and the electrical frequency of the measurement," *Journal of Electronic Materials*, vol. 18, no. 2, pp. 287-292, 1989.

[12] S. Verma and P. Kumar, "Printed Newton's egg curved monopole antenna for ultra wideband applications," *IET Microwaves, Antennas & Propagation*, vol. 8, no. 4, pp. 278-286, 2014.

[13] A. S. Al-Zayed and V. A. Shameena, "A novel FGCPW-fed flag-shaped UWB monopole antenna," *International Journal of Microwave and Wireless Technologies*, available on CJO2015, doi:10.1017/S1759078714001627.

[14] M. Devi, A. K. Gautam and B. K. Kanaujia, "A compact ultra wideband antenna with triple band-notch characteristics," *International Journal of Microwave and Wireless Technologies*, available on CJO2015, doi: 10.1017/S1759078715000409.

[15] I. Messaoudene, T. A. Denidni and A. Benghalia, "A hybrid integrated ultra-wideband/dual-band antenna with high isolation," *International Journal of Microwave and Wireless Technologies*, Available on CJO2015, doi:10.1017/S1759078715000033.

[16] S. Singhal and A. Singh, "Crescent-shaped dipole antenna for ultra-wideband applications," *Microwave and Optical Technology Letters*, vol. 57, no. 8, pp. 1773-1782, 2015.

[17] K. Sawant and C. R. Kumar, "CPW fed hexagonal microstrip fractal antenna for UWB wireless communications," *International Journal of Electronics and Communications*, vol. 69, no. 1, pp. 31-38, 2015.

[18] Y. Zou, X. Zhao, W. Fang and B. Sun, "Design and implementation of a novel dual band notched antenna for UWB applications," *Microwave and Optical Technology Letters*, vol. 56, no. 12, pp. 2922-2925, 2014.

[19] R. Shi, X. Xu, J. Dong and Q. Luo, "Design and analysis of a novel dual band-notched UWB antenna," *International Journal of Antennas and Propagation*, vol. 2014, article ID 531959, 10 pages, 2014.

[20] M. Dorostkar, M. Islam and R. Azim, "Design of a novel super wideband circular hexagonal fractal antenna," *Progress in Electromagnetics Research*, vol. 139, pp. 229-245, 2013.